Supporting Information

Nguyen and Valdivia 10.1073/pnas.1117884109

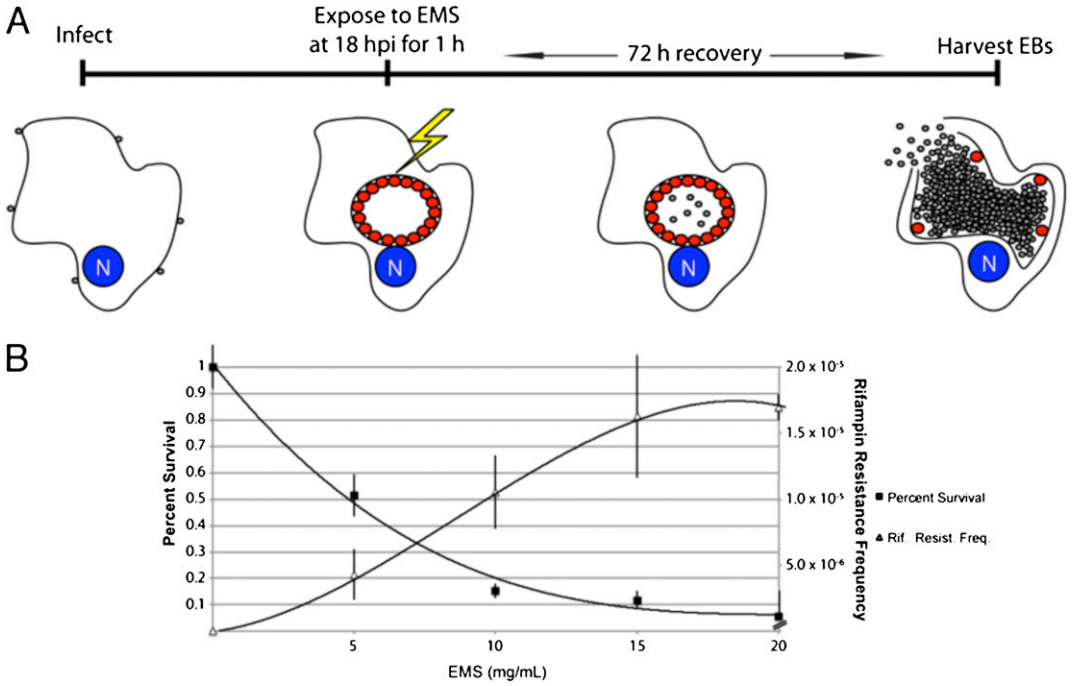

Fig. S1. Effects of EMS treatment on the yield of IFUs and the rate of emergence of rifampin-resistant variants. (*A*) Schematic representation of EMS mutagenesis protocol. *Chlamydia trachomatis* LGV-L2-infected cells were exposed to EMS during the RB stage of the infectious cycle, and the infection was allowed to proceed for 72 h. Mutagenized EB pools were harvested and titered for IFU and plaque-forming units on Vero cells. N, nucleus. (*B*) Monitoring the mutational efficiency of EMS in *C. trachomatis*-infected cells. Total IFUs and rifampin-resistant plaques generated after a 1-h exposure to increasing amounts of EMS were determined. A dose of 20 mg/mL EMS for 1 h led to a ~95% decrease in IFU yields and a >100-fold increase in mutation rates.

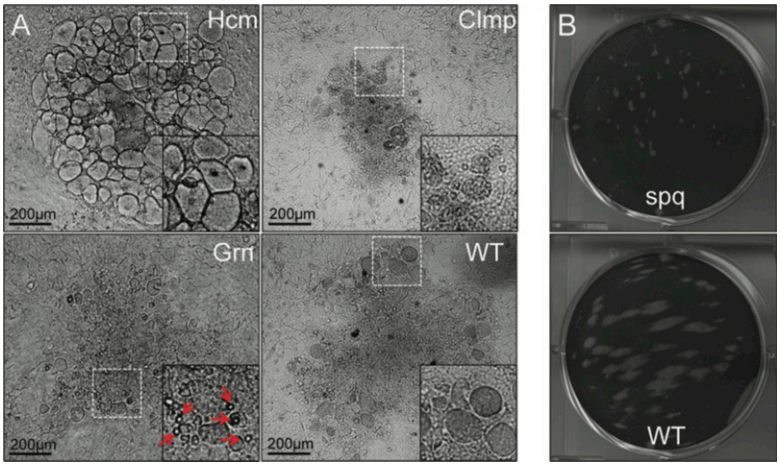

Fig. S2. Emergence of diverse plaque morphologies among EMS-mutagenized *C. trachomatis* variants. A Rif^R variant of *C. trachomatis* LGV-L2 was mutagenized with 20 mg/mL EMS as described for Fig. S1 and allowed to form plaques on Vero cell monolayers. Plaques were visually inspected by day 14, and morphological (*A*) and size (*B*) variants were isolated, amplified in HeLa cells, and used in reinfections of Vero monolayers to confirm the stability of the plaque morphotypes. Examples of common phenotypes are shown including honeycomb (Hcm), clumped (Clmp), small plaque (Spq), and granular (Grn). Arrows indicate large granular deposits within a Grn plaque (see Fig. 2).

Fig. S3. Residues mutated in GlgB among Grn strains are conserved among homologous glycogen-branching enzymes. ClustalW alignment of relevant regions of mammalian, plants, eubacteria, and chlamydial glycogen-branching enzyme homologs. The amino acid changes in GlgB from three independently derived Grn mutants are shown. The GenBank accession numbers for the GlgB proteins are listed in *Methods*. Alignments were generated with the Geneious genome analysis software package. GenBank accession numbers for GlgB were gi189458812, gi146262389, gi16131306, gi297622088, gi269303352, gi15618386, gi29840035, and gi166154212. GlgB sequences were aligned using ClustalW (1) as packaged in the Geneious Pro version 5 software (Biomatters).

1. Thompson JD, Higgins DG, Gibson TJ (1994) CLUSTAL W: Improving the sensitivity of progressive multiple sequence alignment through sequence weighting, position-specific gap penalties and weight matrix choice. *Nucleic Acids Res* 22:4673–4680.

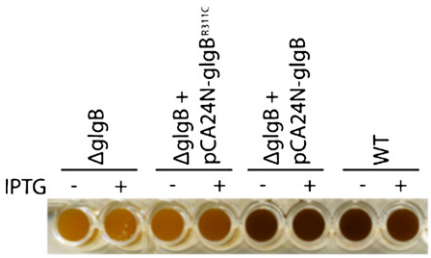

Fig. S4. GlgB^{R311C} failed to complement a glgB deletion in *E. coli*. Pellets from overnight cultures grown in 0.5% glucose in Miller LB were resuspended in iodine solution to detect glycogen. Expression of GlgB in *E. coli* was induced by β-D-1-thiogalactopyranoside (IPTG). The Δ*glgB E. coli* strain stains poorly with iodine compared with the complemented strain (Δ*glgB* + pCA24N-*glgB*) or the wild-type parental strain. The Δ*glgB E. coli* strain expressing the mutant *glgB* (Δ*glgB* + pCA24N-*glgB*^{R311C}) was indistinguishable from the *glgB* deletion strain. The *glgB* deletion strain (Δ*glgB*; JW3395) and the parental wild-type strain (BW25113) were from the Keio collection (1). pCA24N-*glgB* was isolated from the ASKA collection (2) and served as template for site-directed mutagenesis (QuikChange II XL Site-Directed Mutagenesis Kit; Agilent) to generate pCA24N-*glgB*^{R311C} using the following primers: primer 1, GCGCCAACCCGCTGT-TTTGGTACTCGCG; and primer2, CGCGAGTACCAAAACAGCGGGTTGGCGC (underlined nucleotides indicate changes that lead to an R311C amino acid change). Mutations in *glgB* were confirmed by dideoxy sequencing (BigDye; Applied Biosystems). A Δ*glgB* strain was transformed with either pCA24N-*glgB* or pCA24N-*glgB*^{R311C}. For iodine stains, cultures were grown overnight in Miller LB broth supplemented with 0.5% dextrose and/or 0.1 M isopropyl IPTG and 34 μg/mL chloramphenicol. Bacterial pellets were resuspended in an iodine solution (10 mM I_2, 30 mM KI) and imaged.

1. Baba T, et al. (2006) Construction of *Escherichia coli* K-12 in-frame, single-gene knockout mutants: The Keio collection. *Mol Syst Biol 2;* 2006.0008.
2. Kitagawa M, et al. (2005) Complete set of ORF clones of *Escherichia coli* ASKA library (a complete set of E. coli K-12 ORF archive): Unique resources for biological research. *DNA Res* 12: 291–299.

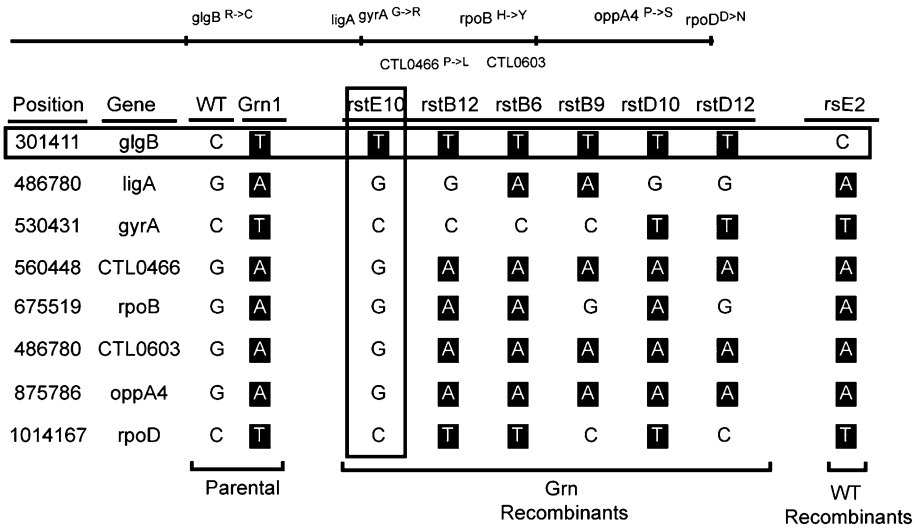

Fig. S5. Genetic linkage between a mutation in *glgB* and the aggregation of glycogen in recombinants derived from crosses with Grn1. Genotypes of recombinant strains derived from a cross between Rif^R Grn1 and a Spc^R strains (rs recombinants), followed by a cross of Grn Rif^{R}Spc^R strains with a Tmp^R strains (rst recombinants) or a wild-type recombinant strain derived from a cross between Grn1 and a Spc^R strain (rs recombinants). The genotypes of recombinant strains were determined by sequencing PCR products flanking mutations identified by WGS. Note that the Grn strain rstE10, where a *glgB* mutation is the only contribution from the parental Grn1 mutant, and the wild-type strain rsE2 strain, where all mutations from Grn1 where present, except for *glgB*, provide definitive evidence that lesions in *glgB* are necessary and sufficient for the mutant phenotype.

Movie S1. Real-time analysis of the accumulation of glycogen aggregates in HeLa cells infected with Grn mutants. Infected cells were imaged over a 20-h period. Note the sudden appearance of glycogen precipitates late in infection for all Grn mutants.

Movie S1